Structure and function analysis of the CMS/CIN85 protein family identifies actin-bundling properties and heterotypic-complex formation

Gabriel Gaidos, Shefali Soni, Duane J. Oswald, Paul A. Toselli and Kathrin H. Kirsch*

Department of Biochemistry, Boston University School of Medicine, 715 Albany Street, Boston, MA 02118, USA

*Author for correspondence (e-mail: kirschk@bu.edu)

Accepted 14 May 2007
Journal of Cell Science 120, 2366-2377 Published by The Company of Biologists 2007
doi:10.1242/jcs.004333

Summary

Members of the CMS/CIN85 protein family participate in clathrin-mediated endocytosis and play a crucial role in maintaining the kidney filtration barrier. The CMS protein structure includes three Src homology 3 (SH3) domains and a proline-rich (PR) region that is connected by a 'linker' sequence to a coiled-coil (CC) domain. We show that CMS is a component of special actin-rich adhesion structures – podosomes – and demonstrate specific actin-binding properties of CMS. We have found that the entire C-terminal half of CMS is necessary for efficient binding to filamentous actin (F-actin). CMS and CIN85 can crosslink F-actin into bundles, a function that depends on the PR region and the CC domain. Removal of these domains reduces migration. CMS can also form heterotypic complexes with CIN85. CIN85 is expressed as multiple isoforms that share the CC domain, suggesting that heterotypic interactions with CMS provides a mechanism to regulate CMS binding to F-actin and thus for modulating dynamic rearrangements of the cytoskeleton.

Key words: Actin bundling, Podosomes, Podocytes, CMS, CD2AP, CIN85, Migration, Coiled-coil

Introduction

Adapter proteins are involved in the intracellular regulation of diverse signaling events of controlling cellular proliferation, differentiation, trafficking, adhesion and motility. The primary function of adapter proteins is to mediate protein-protein and/or protein-lipid interactions. Variations in their distinct domains, and complex homo- and heterotypic interactions, enable the members of the adapter protein family to communicate with other proteins and to build specific spatially and temporally regulated signaling nodes. The recently identified CMS/CIN85 family of adapter-type proteins is involved in orchestrating and regulating receptor tyrosine kinase signaling and cytoskeletal dynamics (Dikic, 2002). The family member CMS/CD2AP/METS-1 ($p130^{Cas}$ ligand with multiple SH3 domains/CD2-associated protein/mesenchyme-to-epithelium transition protein with SH3 domains) (official gene name *CD2AP*, cluster of differentiation 2-associated protein) was independently identified by yeast two-hybrid screens in searching for binding partners for the CD2 receptor (Dustin et al., 1998) and the focal adhesion protein p130Cas (official gene name *BCAR1*, breast cancer antiestrogen resistant 1) (Kirsch et al., 1999), and as a protein induced during kidney development (Lehtonen et al., 2000). The homologue CIN85 (Cbl interacting protein of 85 kDa) (official gene name *SH3K1*, SH3-domain kinase binding protein 1) was first identified by a screen for binding partners of the proto-oncogene product c-Cbl (Take et al., 2000). CIN85 is also known as Ruk (Gout et al., 2000) and SETA (Bogler et al., 2000). For simplification purposes, we refer to the two human homologues of *CD2AP* and *SH3K1* as CMS and CIN85, respectively.

CMS and CIN85 share an identical overall domain structure. The molecules are composed of three N-terminal SH3 domains, followed by a proline-rich (PR) region (providing binding sites for SH3 domain-containing proteins), an unstructured region of approximately 160 residues and a C-terminal coiled-coil (CC) domain that, we have shown, mediates homotypic interaction (Kirsch et al., 1999). The SH3 domains share most similarities among themselves and between family members, and overlapping functions have been identified (Dikic, 2002; Tibaldi and Reinherz, 2003). A growing number of proteins binding to the PR region have been revealed. Previously, we have shown that proteins with different functions bind to this region in CMS, including non-receptor kinases, lipid kinase and adapter proteins, all of which are involved in receptor tyrosine kinase signaling (Kirsch et al., 1999). The discovery of the growth-factor-inducible association of CIN85 and CMS with the E3 ubiquitin ligase Cbl (Take et al., 2000; Kirsch et al., 2001) and the constitutive association with endophilins linked the CMS/CIN85 protein family to the cessation of receptor-induced signal transduction by the endocytic pathway, first shown for CIN85 by Soubeyran et al. and Petrelli et al. (Soubeyran et al., 2002; Petrelli et al., 2002) and for CMS by Lynch et al. (Lynch et al., 2003). This was further supported by the identification of FxDxF motifs in the N-termini of CMS and CIN85 (Brett et al., 2002), which are recognized by AP-2 protein family members of the clathrin complex. CMS is also found in processes involved in post-internalization and endosome formation. We and others have shown that CMS or CIN85 associate with vesicles, to which CMS colocalized with Cbl (Kirsch et al., 2001; Welsch et al., 2005). Recently, a role for a CMS-Cbl-Rab4 complex in

regulating endosome morphology, as well as trafficking to the degradation pathway has been suggested in CHO cells (Cormont et al., 2003). Furthermore, CMS has been found in actin-rich late-endosomal compartments in podocytes (Welsch et al., 2005). The notion that the members of the CMS/CIN85 protein family play a crucial role in the endocytic pathway has been further corroborated by the identification of the association of CIN85 with Alix/AIP1 (official gene name *PDCD6IP*, programmed cell death 6 interacting protein) (Schmidt et al., 2003; Schmidt et al., 2005), synaptojanin-2B1, SHIP-1 and HIP1R (Kowanetz et al., 2004). The CC domains of CMS and CIN85 seem to play an important role in these processes. CC domains are present in many proteins associated with endosomes and the actin cytoskeleton, and it has been reported that actin is required for endocytosis, although its exact role is not yet clear (Kaksonen et al., 2006).

CMS was shown to localize to highly dynamic actin structures at the leading edge of cells and membrane ruffles (Kirsch et al., 1999), and to have a role in cytoskeletal polarization associated with the activation of T cell receptors (Dustin et al., 1998). Subsequently, it has been shown that mice deficient in CD2AP(CMS) die of kidney failure by the age of 6-7 weeks. This is due to a defect in the podocytes. In particular, podocytes lose their specialized actin-rich foot processes, leading to the breakdown of the slit diaphragm, which constitutes the glomerular filtration barrier (Shih et al., 1999). CMS associates with potassium-iodide-sensitive filamentous actin (F-actin) in lysates of purified kidney glomeruli (Yuan et al., 2002). Recently, CIN85 has also been shown to colocalize with F-actin and to have pro-adhesive properties in HEK293 cells (Schmidt et al., 2003). A more versatile role of the CMS and CIN85 proteins in actin dynamics became evident with the discovery of the association of CMS with anillin, a component of the actin-rich cleavage furrow, at the midbody during cell division (Monzo et al., 2005). At the molecular level, CMS is linked to F-actin indirectly by binding to the focal adhesion protein p130Cas and Src-family kinases (Kirsch et al., 1999), cortactin (Lynch et al., 2003), and the CAPZA and CAPZB heterodimer [capping protein (actin filament) muscle Z-line α and β; CAPZ] (Hutchings et al., 2003). Moreover, CIN85 has been shown to bind to the focal adhesion kinase (Schmidt et al., 2003). More recently, Lehtonen et al. (Lehtonen et al., 2002) have shown that CMS binds directly to F-actin. Interestingly, we identified four putative actin-binding motifs in the distal part of CMS (Kirsch et al., 1999). However, knowledge about structural requirements for this interaction is still elusive. To better understand the role of the CMS/CIN85 protein family in cytoskeletal dynamics, we investigated the interaction of CMS and the family member CIN85 with actin.

Here, we present evidence for the localization of CMS to highly dynamic actin-rich adhesion structures, the podosomes. Moreover, we report that CMS and CIN85 bundle F-actin by direct interaction with actin filaments. We provide evidence for structural requirements for this mechanism using biochemical analysis and transmission electron microscopy (TEM). The structural results suggest a common model for the engagement of the CMS/CIN85 family proteins in F-actin bundling, which we show to be important for serum-stimulated cell migration. Moreover, we demonstrate that CMS and CIN85 form a heterotypic interaction via their CC domains, and propose a mechanism where splice variants of CIN85 regulate the bundling activity of the CMS/CIN85 family members.

Results

CMS colocalizes to rapidly changing F-actin structures

To determine the role of CMS in the regulation of the actin cytoskeleton, we compared the subcellular localization of epitope-tagged CMS in NIH 3T3 and COS-7 cells, and in differentiated mouse podocytes. By staining for CMS, we first confirmed that the adapter protein resides in the cytoplasm and is enriched at the membrane, in particular at the leading edge and focal contacts (FCs) – in contrast to paxillin, which is enriched at focal adhesion sites (Fig. 1A). CMS staining at the leading edge was markedly reduced in serum-starved cells as reported (Kirsch et al., 1999) (data not shown). Stimulation of COS-7 cells with the protein kinase C (PKC)-activator phorbol 12-myristate 13-acetate (PMA), mimicking growth factor signaling, resulted in a redistribution of CMS to membrane ruffles, and co-staining with phalloidin demonstrated that CMS colocalizes with newly polymerized actin (Fig. 1B). The distribution of CMS in the cytoplasm was concentrated in small dots similar to those seen by staining for integrins. Interestingly, staining of differentiated podocytes identified, for the first time, the association of CMS with actin-rich rosette-like structures composed of hundreds of podosomes (Fig. 1C). However, we noticed that formation of these structures is an infrequent event in podocytes. To verify that CMS associates with podosomes, we infected NIH 3T3 cells stably expressing activated Src (Src*3T3) with epitope-tagged CMS (Src*3T3/CMS). Podosomes were first described in Src-transformed cells, and staining of Src*3T3 cells with phalloidin, clearly identifies the formation of typical rosettes or ring-like actin-rich podosome structures (Fig. 2A). Immunofluorescence analysis of the Src*3T3/CMS cells demonstrates the accumulation and colocalization of CMS with F-actin in podosomes (Fig. 2A). To further verify these findings, we performed confocal microscopy. As evident from the ventral layer images, CMS localization overlaps with actin in podosome-rich foot processes. These structures stretch towards the dorsal site where lamellipodia become more prominent (Fig. 2B). Moreover, the punctate nature of the podosomes and the colocalization of CMS with F-actin are visible in Fig. 2C. High magnification *z*-axis images revealed that CMS is primarily a component of the podosome core, though it is also present in the podosome ring (Fig. 2C and data not shown). Podosomes are highly dynamic structures, enriched in F-actin, with a turnover time in the order of minutes (Linder and Kopp, 2005), supporting the idea of CMS playing a special role in the formation, stabilization and/or turnover of highly dynamic F-actin structures similarly to FCs. We also investigated the association of endogenous CMS with podosomes by immunofluorescence. Unfortunately, the poor quality of the antibodies available and the low level of expression did not allow us to draw an unequivocal conclusion.

Direct association of CMS with F-actin requires the entire C-terminus

We identified putative actin-binding sites in the C-terminus of CMS that partially overlapped with the CC domain (Kirsch et

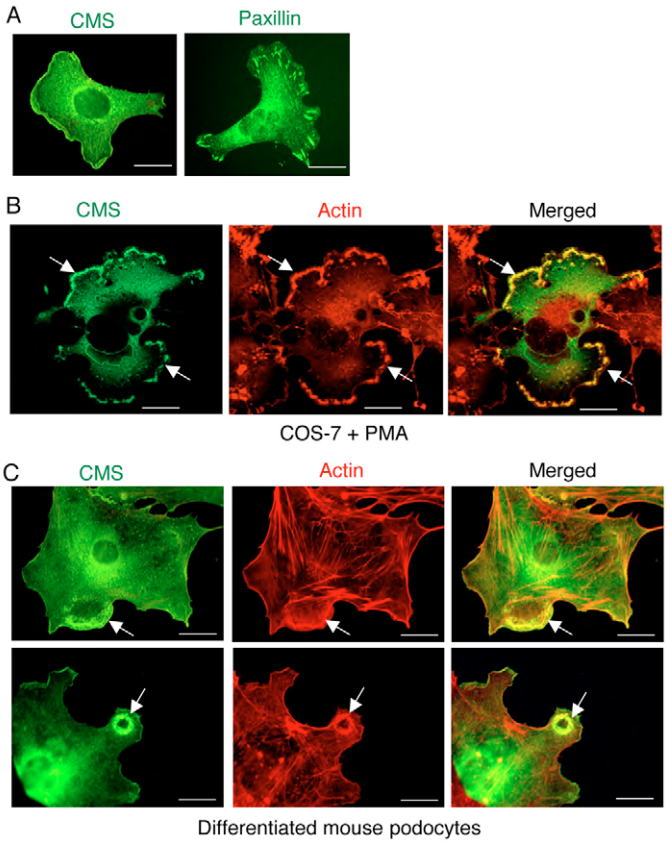

Fig. 1. CMS colocalizes with F-actin to dynamic actin structures such as membrane ruffles and podosomes. NIH 3T3 cells, COS-7 cells and podocytes transfected with CMS, were subjected to immunofluorescence. (A) Endogenous paxillin and transiently expressed FLAG-tagged CMS in NIH 3T3 cells showed a different cellular localization pattern, indicating that the cytoplasmic CMS protein is concentrated at leading edges of migratory cells and not to focal adhesions as seen for paxillin. Bars, 20 μm. (B) COS-7 cells transiently expressing CMS were stimulated with PMA for 10 minutes, stained for CMS and F-actin and analyzed by confocal microscopy. CMS was concentrated and colocalized in prominent membrane ruffles indicated by arrows. Bars, 20 μm. (C) Mouse podocytes stably overexpressing Myc-tagged CMS were differentiated for 7 days and subsequently stained for CMS and F-actin. CMS colocalizes with dynamic actin structures such as lamellipodia and podosomes (see arrows). Bars, 10 μm.

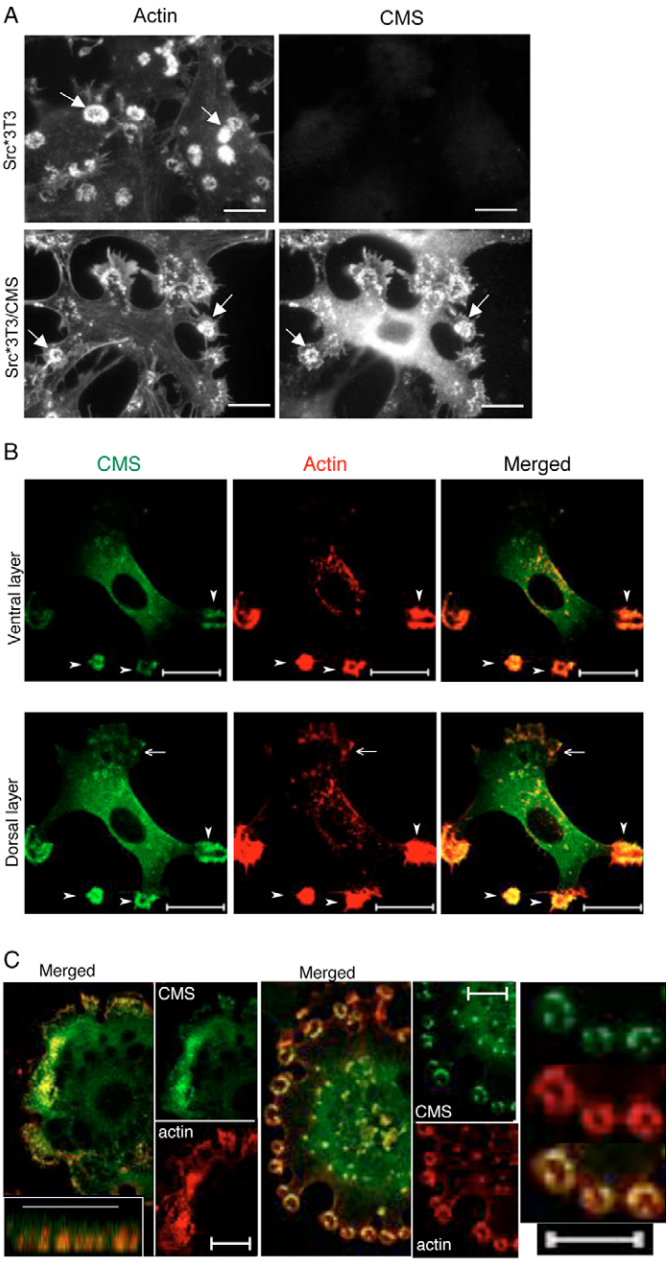

Fig. 2. CMS colocalizes with podosomes. (A) NIH 3T3 cells ectopically expressing activated Src (Src*3T3) were transduced by retroviral infection with vector and vector carrying CMS. Cells were stained for CMS and F-actin and analyzed for subcellular localization. Prominent rosette-like structures composed of individual podosomes are formed in Src*3T3 cells (see arrows), and colocalization of CMS with these structures in Src*3T3/CMS cells is apparent (see arrows). Bars, 20 μm. (B+C) Confocal immunofluorescence microscopy analysis of CMS and actin in Src*3T3/CMS cells. (B) Images were taken at ventral and dorsal layers. Foot processes composed of podosomes are marked with arrowheads, lamellipodia are marked with an arrow. Bars, 20 μm. (C) Images of two cells taken at the ventral layer show prominent podosome clusters. Bars, 20 μm. Inset left: high-magnification *z*-axis images of individual podosomes show localization of CMS to the core; bar, 5 μm.

al., 1999). Such motifs are found in actin-binding proteins, such as α-actinin (F-actin binding), actobindin (actin dimer binding), and thymosin β4 [globular (G)-actin binding]. To determine the minimal sequence requirements necessary and sufficient for CMS to bind actin, we focused on the C-terminal half of CMS. GST fusion proteins of specific deletion mutants were used in in-vitro actin-pull-down assays (Fig. 3A). This assay has been successfully used to analyze the direct interaction of actin with actin-binding proteins. To clarify whether CMS has the capacity to associate with G-actin, we subjected the GST-tagged C-terminus of CMS (CMS CT) to a pull-down assay with actin. G-actin binding was readily detectable in sediment of GST-tagged talin (GST-talin), but no binding was observed with the CMS CT when assays were performed at pH 7.2 and pH 8.0 (Fig. 3B). By contrast, the F-actin binding experiments confirmed that the C-terminus of CMS associates with F-actin (Fig. 3C), indicating that the

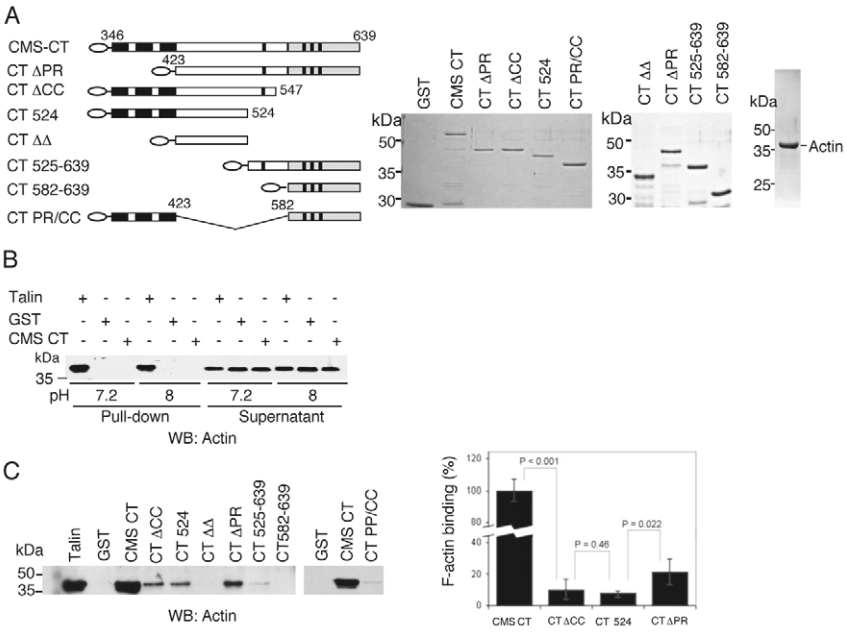

Fig. 3. CMS domains contribute cooperatively to F-actin binding. (A) In order to map the actin-binding site(s) on CMS, a series of CMS deletion mutants fused to GST were purified and used in G- and/or F-actin binding assays. Schematic representation of constructs (black bars represent sequences rich in prolines, white regions represent the linker sequence, gray bars represent the CC domain, black lines mark the locations of the putative actin-binding motifs, ovals represent the GST peptides, numbers mark the first and last aa of the CMS peptides and Coomassie-stained gels of purified GST fusion peptides and G-actin are shown. (B) CMS does not bind to G-actin. G-actin-binding by CMS was assayed in a GST pull-down reaction. The GST peptide, GST-tagged actin-binding domain of talin, and the GST-tagged CMS C-terminus (CMS CT) were incubated with G-actin at different pH conditions, and subjected to pull-down and western blot analysis. (C) Mapping of the F-actin binding domain(s) of CMS. GST-tagged CMS peptides along with GST alone or GST-talin were assayed by F-actin pull-down reactions. Samples were washed and analyzed by western blotting to detect precipitated F-actin (left panel). The graph represents the relative values ± standard deviation (s.d.) of bound F-actin to CMS CT, CT ΔCC, CT 524 and CT ΔPR of three independent experiments (n=3). P values were calculated using Student's t test.

direct association of CMS with actin is restricted to the polymerized form of actin. Moreover, as hypothesized, the CC domain does indeed contribute to the association with F-actin. Removal of this domain reduced the binding by ~90% (P<0.001) (Fig. 3A,C, CTΔCC). Whereas three of the putative actin-binding motifs are situated within the CC domain in the C-terminus, our findings imply that these motifs indeed mediate binding to polymerized actin. A further deletion, including the last remaining putative actin-binding motif, did not lead to a significant further reduction in binding (P=0.46). Interestingly, when we used this identified C-terminal actin-binding region comprising aa 525-639 (CT 525-639, containing all four actin-binding motifs including the CC domain) or the isolated CC domain comprising aa 582-639 (CT 582-639) only weak or no association with F-actin could be measured, which indicates that additional sequences are required for productive F-actin binding. This prompted us to test a construct where we removed the PR region (CT ΔPR). Deletion of the PR region resulted in a similar reduction in binding capacity (~80%) as observed for the CT ΔCC deletion mutant (CMS CT lacking the CC domain). Thus these experiments showed that the PR region is necessary for efficient F-actin binding of CMS. A complete loss of binding was observed when both the PR region and the CC domain were removed (Fig. 3C, CT ΔΔ containing only the 'linker' peptide). In addition, we tested the isolated PR region for binding. Surprisingly, this region was also unable to interact with F-actin (data not shown). Both of the identified binding domains are connected via a peptide sequence of ~160 aa, which we refer to as the 'linker' region. This region is unstructured, and the isolated 'linker' peptide fused to GST (CT ΔΔ) does not associate with F-actin. To determine whether the sole function of this peptide is to link the PR and CC domains of CMS, we generated a GST fusion peptide (CT PR/CC) that connects the PR region directly to the CC domain. Surprisingly, the association with F-actin could not be recovered by this fusion peptide (Fig. 3C), suggesting that the linker domain plays a crucial structural role(s) in CMS binding to F-actin. In summary, these results imply that CMS associates directly with F-actin – for which the PR region and CC domain are necessary but not sufficient – and suggest a synergistic action for both domains and the linker. It would have been of interest to determine the kinetic constant of association, but the unstable nature of the full-length fusion proteins prevented us from making precise calculations.

Like CMS, CIN85 associates directly with F-actin

CMS and the homologue CIN85 share an identical domain structure. However, the putative actin-binding motifs are not found in CIN85. Also, evidence suggests that, in contrast to CMS, CIN85 does not bind actin directly (Tibaldi and Reinherz, 2003; Schmidt et al., 2003), even though it colocalizes with F-actin-rich structures. To determine whether CIN85 associates with F-actin in our in vitro binding assay, we cloned the C-terminus of human CIN85 (CIN85 CT aa 357-665), and tested its ability to interact with F-actin. Moreover, we generated a hybrid construct, where we replaced the 158 aa of CMS linker (aa 423-581) with 158 aa of the CIN85 linker (aa 442-600) (Fig. 4A,B). In vitro F-actin pull-down assays revealed that, in contrast to previous reports (Schmidt et al., 2003), the CIN85 CT does bind directly to F-actin (Fig. 4B, middle panel). However, CIN85 CT binding to F-actin was consistently weaker throughout the experiments (Fig. 4B). Furthermore, whereas the CMS CT ΔPR peptide retained 30% of the CMS CT actin-binding capacity, actin-binding of CIN85 CT ΔPR was almost completely lost although the CC domain was present (Fig. 4C). This difference might indeed be due to the presence of the putative actin-binding motifs in CMS.

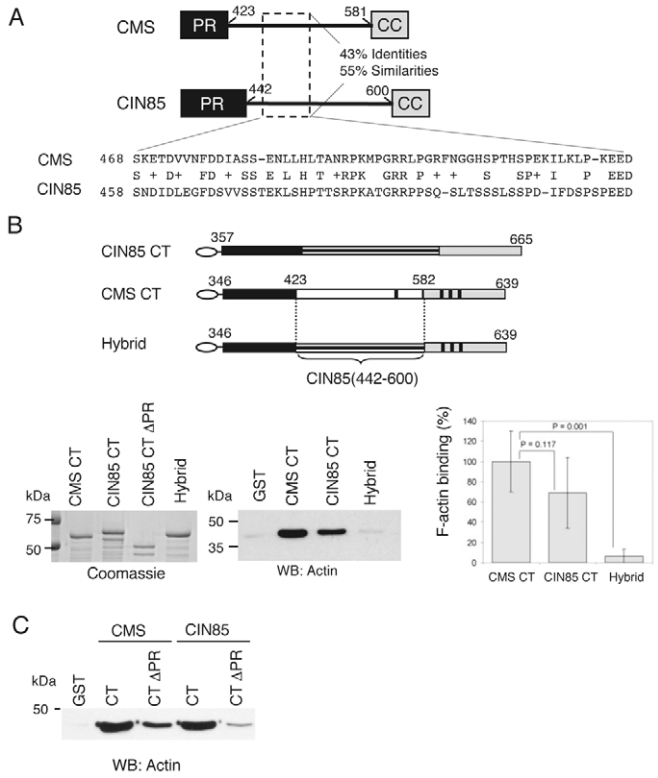

Fig. 4. The CMS linker region plays a crucial role in maintaining the actin-binding activity of CMS. (A) The linker sequences of CMS and CIN85 were aligned using the BLAST program. Schematic representation of the C-terminal half of CMS and CIN85 depicting the region of identified similarities (boxed area). Sequence alignment of this region is shown below. Black bars represent the PR regions, gray bars represent the CC domain, solid lines mark the linker sequence. (B) Schematic representation of CMS CT in relation to the C-terminus of CIN85 (CIN85 CT), and a hybrid peptide of the C-termini of CMS and CIN85 (Hybrid), in which the linker sequence is replaced by the corresponding sequence of CIN85 (domains in CMS are depicted as in Fig. 3A; black rectangle in CIN85 CT represent sequences rich in prolines, striped rectangle represents linker sequence). Depicted GST-tagged peptides were purified, analyzed using Coomassie-stained acrylamide gels (left panel), and assayed for F-actin-binding activity in GST pull-down reactions. GST was included as a negative control. The reactions were subjected to western blot analysis to score for bound actin. Summary of relative values ± s.d. of actin-binding represents the average of four independent experiments (n=4). P values were calculated using Student's t-test. (C) The PR region of CIN85 contributes to actin-binding. Indicated GST-tagged peptides or GST alone were assessed for F-actin-binding in pull-down reactions. Reactions were analyzed as described.

Productive F-actin-binding by CMS depends on specific sequence requirements of the linker region

The lack of actin-binding of the linker, made it suitable for swapping experiments to test whether correct spacing and/or specific sequences are required for CMS to bind to actin. Surprisingly, replacement of the CMS linker with the CIN85 linker (Hybrid) resulted in a complete loss of actin-binding, suggesting that the linker of CMS, and CIN85 as well, may not merely function as a connector of the two actin-binding domains (Fig. 4B, middle panel). Instead, the linker sequence

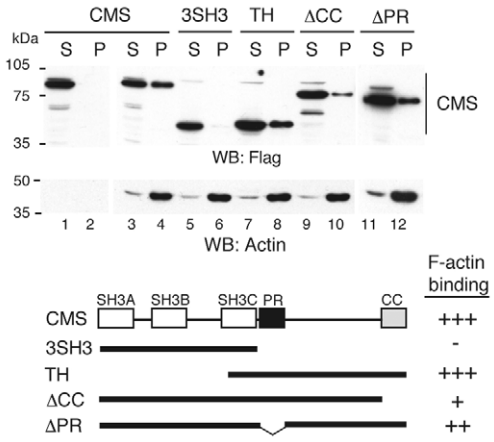

Fig. 5. CMS binding to F-actin in whole-cell extracts mirrors the binding measured with purified components. Cell lysates from 293T cells expressing the FLAG-tagged CMS constructs depicted in the scheme were incubated with exogenous F-actin and tested for their ability to co-sediment (lanes 3 to 12). F-actin was sedimented by centrifugation at 100,000 ***g***. The soluble (S) and actin-bound fractions (P) were resolved by SDS-PAGE and analyzed by western blot for the presence of F-actin and CMS. Lanes 1 and 2 represent negative controls without F-actin. The CC domain and PR region deletion mutants of CMS show a diminished F-actin binding activity, similarly to the results of GST pull-downs assays (Fig. 3). F-actin-binding was scored: +++, strong; ++, medium; +, low; –, no binding.

may contain information regarding correct spatial assembly. Moreover, it might help stabilize the binding to F-actin. Comparison of the CMS and CIN85 linker sequences identified 55% similarities in only a short stretch of 54 aa, whereas the entire linker is composed of ~160 aa (Fig. 4A). These results further suggest that productive F-actin-binding depends on specific sequence requirements for the linker region.

The N-terminal SH3 domains do not contribute to the actin-binding capacity of CMS

Next, we studied the contribution of the PR region and the CC domain for F-actin binding in the context of the full-length molecule in whole-cell extracts. In addition, we investigated the actin-binding capacity of the SH3 domains. For this purpose, we expressed FLAG-tagged full-length CMS and deletion mutants CMS 3SH3, CMS ΔCC and CMS ΔPR (Fig. 5B) and a GFP-talin control (not shown) in 293T cells. Lysates of transfected cells were incubated with exogenously supplied F-actin, and the ability of the individual FLAG-tagged constructs to co-sediment with F-actin by high-speed centrifugation was examined by immunoblotting (Fig. 5). In the absence of F-actin no tagged CMS protein was found in the pellet. However, addition of F-actin resulted in a significant shift of the full-length CMS protein into the pellet. By contrast, there is no detectable sedimentation of the N-terminal peptide (CMS 3SH3) suggesting that the SH3 domains are unable to link CMS directly or indirectly to filamentous actin. Moreover deletion of the PR region and CC domain reduced the sedimented amount of CMS comparable with the reduced binding detected in the GST pull-down assays. These results corroborate our previous data and further suggest that both, PR region and CC domain are necessary for efficient interaction

of CMS with F-actin. Furthermore these data suggest that the SH3 domains do not participate in F-actin binding.

CIN85 hetero-oligomerizes with CMS via the CMS CC domain

CC structures are implicated in homotypic and heterotypic protein-protein interactions. Recently, we and others have demonstrated that CMS and CIN85 can homo-oligomerize via their CC domain (Kirsch et al., 1999; Borinstein et al., 2000). To determine whether CMS and CIN85 can form hetero-oligomers, we expressed full-length FLAG-tagged CMS and mutants with progressive deletions of the CC domain in 293T cells (Fig. 6A, right panels, and 6E). Pull-down experiments using GST-tagged CIN85 CT and 293T cell lysates overexpressing CMS revealed that CIN85 associates with CMS (Fig. 6A, left panel). Complete deletion of the CMS CC domain

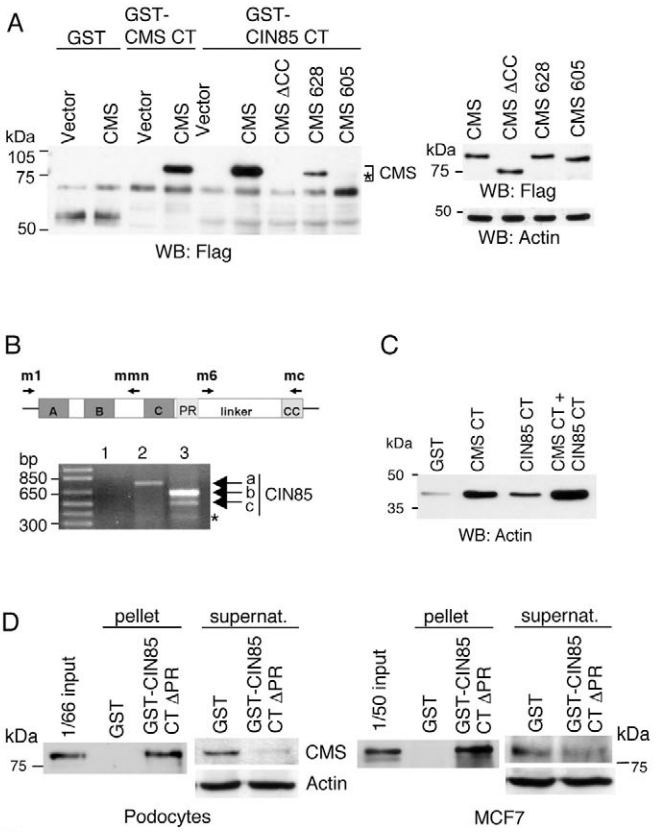

Fig. 6. Heterotypic oligomerization of CMS with CIN85 mediated by the CC domain. (A) Lysates from 293T cells transiently expressing wild-type Flag-tagged CMS, deletion constructs (CMS ΔCC, CMS 628 CMS 605; positions of the introduced stop codons are marked with triangles in panel E), and vector control were incubated with 10 μg purified GST-CIN85 CT. Similarly, control and CMS expressing lysates were incubated with GST and GST-CMS CT (negative and positive controls, respectively). Precipitates were analyzed by western blotting with FLAG antibody (left panel), equal expression of the CMS constructs is represented in the right panels. (B) Expression of endogenous CIN85 in mouse podocytes. PCR was performed on cDNA generated from randomly growing immortalized mouse podocytes. Amplification of the 5′ region of CIN85 was performed with mouse-specific primer m1 (positioned in exon 1) and mmn (positioned in exon 9) lane 2. Amplification of the 3′ region of CIN85, including the CC domain, was performed with primer m6 (positioned in exon 19) and mc (positioned in exon 24) lane 3. PCR primers m1, mmn and mc are as described (Buchman et al., 2002). Amplified and sequenced cDNAs (a, b, c) are indicated with arrows; a, 5′ region of CIN85; b, full-length 3′ region of CIN85; c, 3′ region of CIN85 Δ exon 21; *, additional amplified cDNA of unknown nature; lane 1, negative control. (C) An additive effect on actin-binding was observed when CMS and CIN85 were combined in one reaction (protein ratio 1:1). Pull-down assays performed with the indicated peptides were analyzed as described above. (D) Binding of endogenous CMS to CIN85 CT ΔPR. Whole-cell extracts (1.5-2 mg) of podocytes and MCF-7 cells were incubated with GST or GST-CIN85 CT ΔPR and analyzed by western blotting for association with CMS (pellet). Equal amounts of supernatant (supernat.) were loaded and analyzed for CMS and actin. (E) CMS/CIN85 family sequence alignment (different species) of the distal C-terminus containing the CC domain performed with the Clustal W program. Conserved amino acids are color-coded (red, small and hydrophobic; blue, acidic; magenta, basic; green, hydroxyl, amine or basic-Q residue). Consensus symbols are depicted (*, identical residues; :, conserved substitutions; ., semi-conserved substitutions). Coiled-coil probabilities are given for the CMS/CIN85 family members [Paircoil program, Berger et al. (Berger et al., 1995)].

E

Species	Protein name	Amino Acid Sequence	Accession #
CMS deletion mutants		582 ∇ 605 ∇ 628 ∇ 639	
CHICKEN	HYPOTHETICAL PROTEIN	SVEEL RAQIQDL MNLVDAL RKEHGRE LEKLRKD LEEEKLM RSNLEIE IEKLKKA VMST	CAG31983
DOG	CD2AP	SLDEL RAQITEL LCIVDAL KKDHGKE LEKLRRE LEEEKAM RSNLEVE IAKLKKA VLLS	XP_532162
MOUSE	CD2AP/METS-1	SVDEL RAQIIEL LCIVDAL KKDHGKE LEKLRKE LEEEKAM RSNLEVE IAKLKKA VLLS	NM_009847
RAT	CD2AP	SLDEL RAQIIEL LCIVEAL KKDHGKE LEKLRKD LEEEKAM RSNLEVE IEKLKKA VLSS	NM_181475
ORANGUTAN	CD2AP	SLDEL RAQIIEL LCIVEAL KKDHGKE LEKLRKD LEEEKAM RSNLEME IEKLKKA VVSS	CAH91263
HUMAN	CMS/CD2AP	SLDEL RAQIIEL LCIVEAL KKDHGKE LEKLRKD LEEEKTM RSNLEME IEKLKKA VLSS	NM_012120
CMS/CD2AP coiled-coil probability		---------40%-----|--77%--|-------------------100%-----------------|	
Coiled-coil heptad register		abcdefg abcdefg abcdefg abcdefg abcdefg abcdefg abcdefg abcd	
CIN85 coiled-coil probability		--------------60%----|----------------------100%-----------------|	
HUMAN	CIN85	AVEEL RTQVREL RSIIETM KDQQKRE IKQLLSE LDEEKKI RLRLQME VNDIKKA LQSK	AF230904
RAT	Ruk/SETA	AIEEL RTQVREL RSIIETM KDQQKRE IKQLLSE LDEEKKI RLRLQME VNDIKKA LQSK	AF255888
MOUSE	SH3KBP1	AIEEL KMQVREL RTIIETM KDQQKRE IKQLLSE LDEEKKI RLRLQME VNDIKKA LQSK	AH011510
DOG	SH3KBP1	AVEEL KMQVREL RTIIETM KDQQKRE IKQLLSE LDEEKKI RLRLQME VNDIKKT LQSK	XP_858606
CATTLE	SH3KBP1	AMEEL RTQVREL RSIIETM KDQQKRE IKQLLSE LDEEKKI RLRLQME VNDIKKA LQSK	XP_587629
CHICKEN	SH3KBP1	ALEEL RTQVKEL RTIIETM KDQQKKE IKQLLSE LDEEKKI RLRLQME VNDIKKA LQSK	NP_001025976
XENOPUS	LOC445851 protein	EMDDL KAQISDL LSIVHAL RKEHRKE MDHLKKQ LDEERLL RTHLETE VDKLKKA VQ	AAH97671
PUFFERFISH	UNNAMED	TLEEL KNQLRDL RASVELL KSQHRQE VRQLSSA LDEEKKM RISLQVR TN	CAG05454
Consensus		:::* : *: :* :. : :.:: :* : :* *:**: : * *: . : .:**: : .	

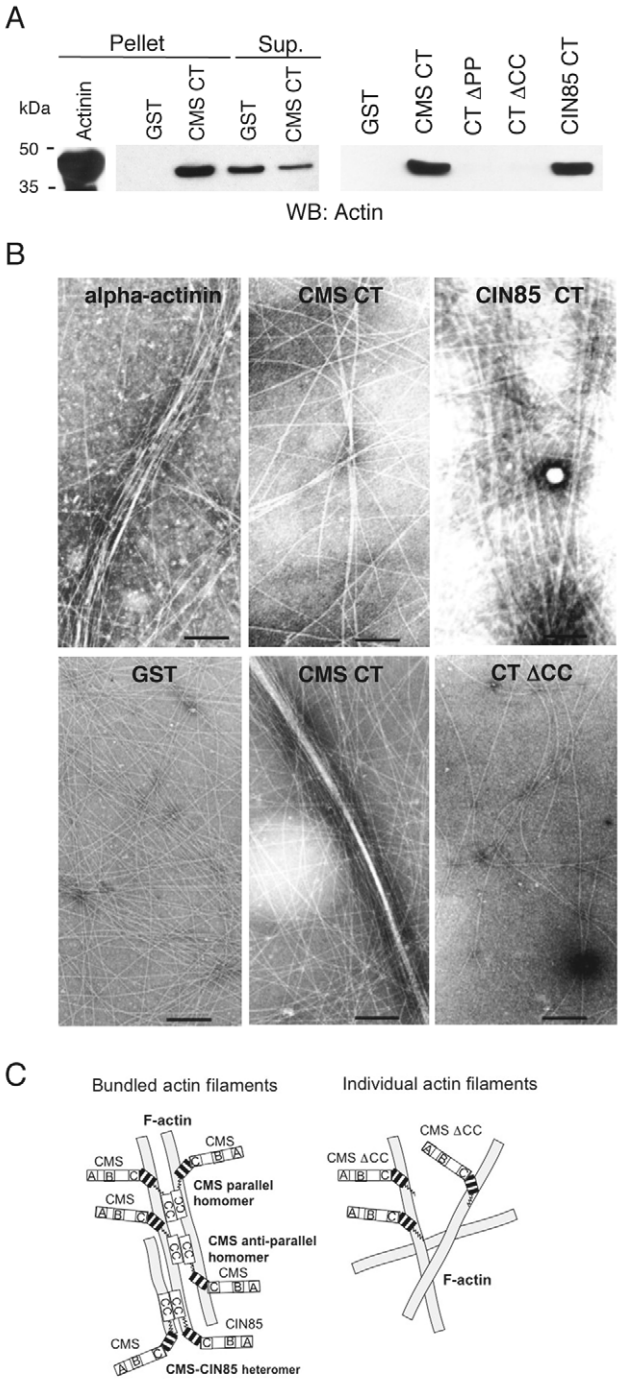

Fig. 7. CMS and CIN 85 crosslink individual F-actin filaments into bundles. (A) Biochemical actin bundling assay. Freshly polymerized non-muscle actin was incubated for 30 minutes with α-actinin, GST and CMS CT (left panel), or with GST, CMS CT, CT ΔPR, CT ΔCC and CIN85 CT. The F-actin bundles were separated from soluble F-actin filaments by centrifugation, and the pellets were subjected to western blot analysis. CMS CT and CIN85 CT caused actin pelleting, with a detectable depletion of the actin amount in the CMS CT supernatant. (B) TEM of negatively stained preparations of actin filaments and F-actin crosslinked by CMS CT and α-actinin. F-actin bundles formed when freshly polymerized, non-muscle F-actin was incubated with CMS CT, CIN85CT or α-actinin (positive control). The CC domain is crucial for the formation of actin filament crosslinks, because in the presence of CMS ΔCC no bundles were formed similarly to GST (negative control). Bars, 100 nm. (C) These findings allow us to propose a model for the interaction of CMS with F-actin. The CC domain plays a dual role: being important in actin binding and filament crosslinking.

resulted in a loss of this association indicating that the CC domain is necessary for binding of CIN85 to CMS. This is underscored by the finding that progressive deletion of the CC domain also progressively reduced the interaction of CIN85 with CMS (Fig. 6A). These results imply that a heterotypic interaction is indeed mediated by a higher order CC interaction. Thus, we have for the first time demonstrated that members of the CIN85/CMS family form heterotypic complexes.

Podocytes express full-length CIN85 and variants

Expression analysis of CIN85, by using the RT-PCR established by Buchman et al. (Buchman et al., 2002) to identify full-length CIN85 and variants, revealed that the full-length form of CIN85 is expressed in immortalized mouse podocytes (Fig. 6B). Therefore, CMS and CIN85 are expressed in the same cell type suggesting that a heterotypic interaction also occurs under physiological conditions. Interestingly, when we assessed actin binding of the CMS CT and CIN85 CT in one reaction, we found that the two proteins neither compete nor interfere with the binding of the other partner in vitro (Fig. 6C). While the full-length C-terminus of CIN85 was the major amplified form, we noticed the amplification of two CIN85 C-terminal variants of approximately 550 bp and 350 bp (Fig. 6B, lane 3). We have confirmed that the longer variant lacks exon 21, resembling the $CIN85_{h3}$ isoform described by Buchman and colleagues (Buchman et al., 2002). Deletion of exon 21 removes a portion of the CIN85 linker region, but it keeps the CC domain intact, suggesting that this variant of CIN85 is also able to form heterotypic complexes with CMS, but might interfere with F-actin-binding. To begin to elucidate whether endogenous CMS has the potential to associate with the short forms of CIN85, we precipitated endogenous CMS from podocyte and human MCF-7 breast cancer cell lysates with GST-tagged CIN85 CT ΔPR (resembling native $CIN85_t$) (Buchman et al., 2002). In both cases, and under high-stringency and low-stringency conditions, CMS was bound to CIN85 CT ΔPR (Fig. 6D), further supporting the notion that endogenous CMS forms heterotypic complexes with CIN85 variants.

We used the Clustal W algorithm to align sequences of the CC domains of different species of the CMS/CIN85 family. This analysis revealed extensive sequence homology within the species of CMS, as well as CIN85. In addition, considerable homology is also evident within the CMS/CIN85 family, which is summarized by the consensus in Fig. 6E. The CC domains of the CMS and CIN85 members follow the heptad pattern, in which the ‘a’ and ‘d’ positions within a heptad repeat are most crucial for homo- and heterotypic oligomerization. Interestingly, these residues are among the most conserved (within the five complete heptads that fall into the 100% probability, all of the ‘a’ and ‘d’ positions are at least conserved substitutions, while 60% are identical), supporting our finding that CMS and CIN85 form heterotypic interactions for which the CC structure is crucial.

CMS and CIN85 bundle F-actin in vitro

F-actin-binding proteins that carry multiple actin-binding domains or that can dimerize have been shown to mediate actin filament bundling (Matsudaira, 1991). Consequently, we asked whether CMS is able to bundle actin filaments. Crosslinked actin filaments can be separated from individual filaments by low-speed centrifugation. In the presence of CMS CT, F-actin was pelleted as determined by immunoblotting. This indicates the formation of crosslinked actin filaments (Fig. 7A, left panel), which also led to a partial depletion of F-actin in the supernatant fraction. In the presence of GST alone F-actin was not pelleted. α-actinin was used as a positive control. We next tested whether bundling activity is a common characteristic for the CMS/CIN85 protein family by including the CIN85 CT peptide in the bundling assay. Moreover, we asked whether deletion of one of the identified CMS actin-binding regions has an effect on the bundling ability. Indeed, the experiments revealed that CIN85 bundles F-actin as efficiently as CMS CT, and deletion of either the PR region or the CC domain of CMS completely abolished formation of F-actin bundles (Fig. 7A, right panel).

Additionally, transmission electron microscopy (TEM) was used to corroborate the results obtained in the bundling assay. TEM experiments clearly show that the C-termini of CMS and CIN85 have the capacity to bundle F-actin (Fig. 7B). Defined F-actin bundles were visible in the presence of the CMS CT or CIN85 CT constructs, similar to the bundles seen in the samples containing α-actinin. However, the bundles formed in the presence of CMS CT or CIN85 CT appeared to be more tightly packed compared with actinin, as presented in view fields of two different areas. Interestingly, the CMS ΔCC construct did not induce bundle formation, consistent with the results obtained in the biochemical bundling assay and, thus, underscores the fact that F-actin crosslinking requires at least two actin-binding surfaces as depicted in the model (Fig. 7C). In summary, these in vitro results provide evidence that CMS and CIN85 bind and bundle actin filaments, and this requires at least two independent actin-binding surfaces.

A functional CC domain is required for cell migration

As we have shown, CMS is concentrated in podosomes and at the leading edge of cells. We hypothesized that aberrant expression of CMS disturbs actin dynamics and thus induces changes in cell migration. To explore the importance of CMS in cell migration, we first used an siRNA approach to downmodulate the expression of endogenous CMS in podocytes. Reduction in CMS expression resulted in 40-45% reduced serum-stimulated migration (Fig. 8A). To analyze the role of the C-terminal actin-binding sub-domains of CMS in migration, we used podocytes expressing Myc-tagged CMS and mutants lacking either the CC domain (CMS ΔCC) or the PR region (CMS ΔPR) in a Boyden chamber assay. Interestingly, migration of podocytes expressing CMS ΔCC was significantly reduced by ~40% (P<0.01) at 4 hours post-plating (Fig. 8B), when compared with vector containing control cells. Deletion of the PR region resulted in an attenuated migration. However, the effect was less pronounced (P=0.056). These results were corroborated with Src*3T3 fibroblasts, in which the migration of Src*3T3 ΔCC and Src*3T3 ΔPR cells was significantly reduced by >35% and 15% (P<0.0001 and P<0.002, respectively) at 2 hours post-plating (Fig. 8C). CMS plays a role in cell migration, and deletion of the CC or PR domain might interfere with the spatial and temporal assembly of larger protein complexes, and with the coupling of integrins to the actin cytoskeleton required for migratory processes.

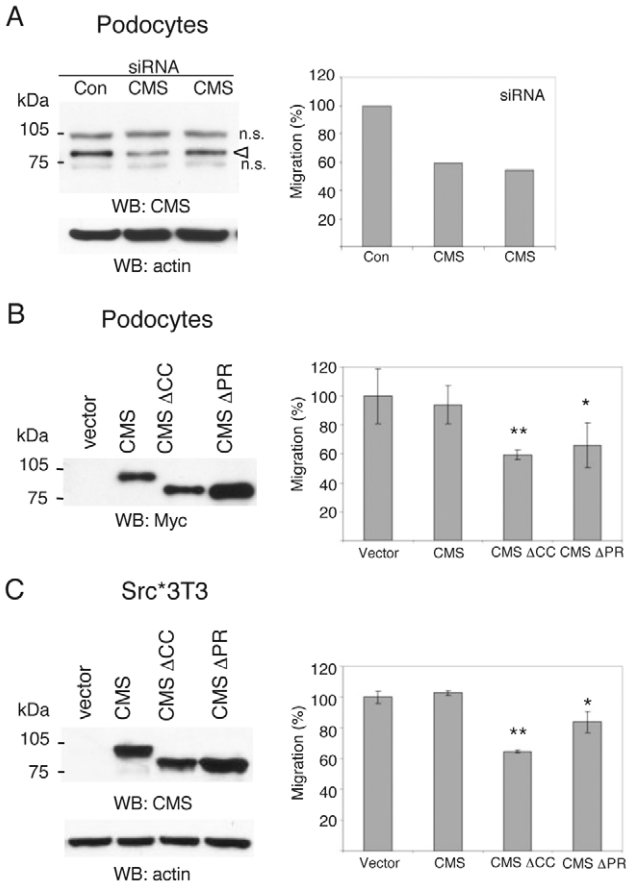

Fig. 8. The CC domain and PR region are important for cell migration. (A) Podocytes were transfected with two different concentrations of CMS siRNA or control siRNA in triplicate. After 48 hours cells were subjected to serum-stimulated Boyden chamber migration assay. Cell lysates were analyzed by western blotting for CMS and actin. (B) Podocytes expressing mutated forms of CMS display reduced migration. Cells stably expressing CMS, CMS ΔCC, CMS ΔPR or vector control were subjected to a serum-stimulated migration assay for 4 hours. Data represent the mean ± s.d. of triplicates from three independent experiments (n=3; right panel; *P<0.01; **P=0.056). (C) Transformed NIH 3T3 cells display reduced migration. Src*3T3 cells expressing the indicated peptides were subjected to a serum-stimulated migration assay for 2 hours. Data represent the mean ± s.d. of triplicates from three independent experiments (n=3; *P<0.0001; **P<0.002). P values were calculated using Student's t test. Protein expression was determined by western blot analysis.

Discussion

The CMS/CIN85 family has been implicated in receptor-mediated endocytosis, in particular in bridging Cbl-bound activated tyrosine kinase receptors to clathrin/AP complexes via the interaction with endophilins (Soubeyran et al., 2002; Petrelli et al., 2002; Kobayashi et al., 2004). This endocytic pathway is a multistep process, in which a role for the actin

cytoskeleton has been implicated. It has been shown that CMS is concentrated in dynamic actin structures that form in response to growth factor binding to their respective receptors, and in dot-like structures throughout the cytoplasm (Kirsch et al., 1999; Welsch et al., 2001). In this study, we identified CMS as a molecular component of podosomes, which are highly dynamic actin-rich adhesion structures mostly studied in motile cells such as osteoclasts and macrophages (Marchisio et al., 1987; Ochoa et al., 2000). Unlike focal adhesions, podosome clusters assemble and disassemble within minutes in a process involving the rapid polymerization and depolymerization of the central actin core (Destaing et al., 2003; Buccione et al., 2004). Based on our studies, CMS colocalizes with filamentous actin throughout the podosome belt, which is formed by individual podosomes clustered into rosette-like structures. The fact that CMS colocalized to the podosomal core is in line with our hypothesis that CMS plays a crucial role in dynamic actin processes. They are further corroborated by recent reports showing that several CMS/CIN85-binding proteins, including Cbl, endophilin, Src and cortactin are found in the same prominent podosome clusters observed in transformed BHK21 cells and in osteoclasts (Ochoa et al., 2000; Bruzzantini et al., 2005), and by the very recent report by Nam et al. (Nam et al., 2007) showing CIN85 localization to invadopodia. It is feasible that some of the highly dynamic actin structures that do not colocalize with endosomal markers (Welsch et al., 2005), and the dot-like structures observed by us previously (Kirsch et al., 1999), are identical to individual podosomes. These findings further underscore the notion that CMS plays an active role in regulating cytoskeletal changes.

Interestingly, Lehtonen et al. recently showed that CMS binds F-actin directly by using purified components (Lehtonen et al., 2002). However, no specific domain had been ascribed to this function. By performing extensive mapping studies, we revealed that direct binding of CMS to filamentous actin depends on structural information provided by the entire C-terminal half of the protein. Though we demonstrated that the PR and linker regions, as well as the CC domain of CMS, are necessary for actin binding, the isolated domains failed to interact with F-actin. Only when the linker region was connected to either peptide, actin-binding was partially restored. Nevertheless, full actin-binding, was achieved only if the overall structure of the C-terminus was maintained, indicating that additional factors, such as spatial properties, play an important role. Of importance is specific sequence and structural information of the linker region, as evident from the experiments with the hybrid peptide. It seems that the CMS linker-sequence contains information that is not present in CIN85, a fact also evident from the sequence alignment of CMS and CIN85. Interestingly, data obtained with whole-cell extracts mirror the results from the pull-down experiments. This underscored the importance of the integrity of the C-terminus. Our findings are similar to the actin-binding mechanism of CORO1A (also known as coronin-like protein p57), a member of the coronin family. F-actin-binding of CORO1A through the C-terminus (CT, 297-461) requires a functional leucine zipper situated in a short dimerization/trimerization domain (CC, 432-461) (Liu et al., 2006). In addition to the direct F-actin binding, coupling of CMS or CIN85 to F-actin via cortactin (Lynch et al., 2003), Alix/AIP1 (Chen et al., 2000), or CapZ (Hutchings et al., 2003) adds a layer of complexity and probably regulation. The indirect associations, e.g. with the capping protein CapZ, may have consequences for dynamic actin-polymerization processes (Bruck et al., 2006), whereas the direct binding of CMS or CIN85 to F-actin may facilitate this process by stabilizing the CMS-CIN85-actin complex.

Although we had speculated that the CC domain and the putative actin-binding motifs are important for direct interaction with F-actin, our experiments with CIN85 suggest that, although these motifs support binding of CMS, they are not necessary. We have shown that CIN85, which does not contain any of those motifs, binds to F-actin almost as efficiently as CMS, suggesting that the overall tertiary structure is the primary determinant for binding. Nonetheless, CMS binding to F-actin was more efficient than CIN85 binding, which became more prominent after deletion of the PR region in both adapters. The difference in actin-binding efficiency may indeed be due to the presence of the putative actin-binding motifs in CMS. Owing to the instability of the full-length CMS CT and CIN85 CT, fully quantitative methods could not be used to determine the actin-binding Kd of these peptides. It has been reported that CIN85 colocalizes with F-actin (Schmidt et al., 2003; Hutchings et al., 2003). However, Schmidt et al. were unable to detect any direct association of CIN85 with F-actin in immunoprecipitates using lysates of primary cortical rat astrocytes (Schmidt et al., 2003). Consequently, they proposed an indirect contact of CIN85 with F-actin through Alix/AIP1 or cortactin. By contrast, our results provide the first evidence that CIN85, similar to CMS, makes direct contact with F-actin. In our assays, we used purified components, including F-actin, which was polymerized under controlled conditions, and which may explain the different result. Furthermore, F-actin-binding may vary depending on the physiological state of the cells. We noticed that with prolonged polymerization actin-binding increased. Nonetheless, indirect association of the CMS and CIN85 proteins with F-actin through cortactin, Alix/AIP1 or other molecules might enable a mechanism for further temporal and spatial regulation. Overall, our data suggest a general actin-binding mechanism for proteins of the CMS/CIN85 family.

CMS and CIN85 can also interact with each other via their CC domain. The functional implication here is that CIN85 isoforms may regulate the actin-bundling activity of CMS and of full-length CIN85. The mouse locus transcribes into at least 12 alternative isoforms, which translate into seven principal CIN85 variants (Buchman et al., 2002). Four variants – $CIN85_t$, $CIN85_{\Delta CP}$, $CIN85_h$, and $CIN85_s$ – are potential negative regulators. They contain an intact CC domain, thereby maintaining their oligomerization properties, but have lost the PR region and other domains including portions of the linker. Consequently, homotypic and heterotypic interaction might regulate the interaction with F-actin and the assembly of specific multiprotein complexes. In fact, $CIN85_t$ resembles the CIN85 ΔPR and CMS ΔPR constructs, and $CIN85_h$ resembles CT 525-639, all had significantly reduced actin-binding activity. Not many data are currently available regarding the regulation of the isoforms and their in vivo expression, but our findings warrant further investigation.

Our final experiments demonstrated that CMS and CIN85 bundle F-actin in vitro. Actin-bundling proteins contain

multiple actin-binding surfaces per monomer, which is consistent with our findings for CMS and CIN85. However, the bundling model we present here is preliminary, and requires further investigation for a more detailed understanding of its exact mechanism. It is feasible that CMS oligomerizes in antiparallel fashion, as known for α-actinin and ABP-120 (Matsudaira, 1991). Moreover, the binding domains might not attach to the same rather to different actin filaments, thereby obviating oligomerization as condition for crosslinking. All of this will have an influence on how tightly packed the bundles are, because spacing of the actin-binding sites is a critical determinant (Meyer and Aebi, 1990).

Prominent reorganization of the actin cytoskeleton occurs during processes of cell adhesion and migration. The cells most noticeably affected by targeted deletion of CMS are podocytes (Shih et al., 1999), but ectopic expression of CMS did not cause visible changes in the actin cytoskeleton of the cells. This may be due to the fact that our immunofluorescence studies are end-point experiments, and early dynamic adhesion and migration processes are not captured by this method. Nonetheless, the reduced migration observed in podocytes with downmodulated CMS or podocytes expressing CMS ΔCC and CMS ΔPR underscores a role for CMS in actin dynamics associated with cellular motility. The stronger effects observed with the CMS ΔCC construct might be due to the fact that this molecule lost the ability to interact with endogenous CMS/CIN85. By contrast, CMS ΔPR can form oligomers with wild-type CMS or CIN85 proteins, and these heteromeric mutant-wild-type complexes might partially alleviate the inhibitory effect.

Overall, the effects of the CMS mutants on the actin cytoskeleton in podocytes are moderate. This might be due the fact that these podocytes express high levels of endogenous CMS, or other actin-binding proteins including CIN85, which may compensate. The large number of known actin-binding proteins with partially overlapping functions provides the cells with a robust backup system. As seen for villin-deficient mice, lack of villin has no noticeable effect on the ultrastructure of the microvilli, unless the system is stressed (Ferrary et al., 1999). Thus it is possible that CMS or CIN85 are not required as actin-bundling proteins per se but are important when cells or tissues are physiologically challenged. Interestingly, we observed in COS-7 cells transiently expressing CMS disappearance of stress fibers, and appearance of thick, short dot-like F-actin structures (G.G. and K.H.K., unpublished). The mechanisms are not clear but, in contrast to podocytes, COS-7 cells are highly transformed cells and have increased tyrosine kinase activities. The results described here establish a new direct link between the actin cytoskeleton and cell migration. Further studies are necessary to determine the extent to which CMS and CIN85 proteins are involved in the regulation of cellular processes associated with the cytoskeleton.

Materials and Methods

Cell lines and culture

COS-7 cells and human 293T kidney epithelial (293T) cells were cultured and transiently transfected as described previously (Kirsch et al., 1999). NIH 3T3, Src*3T3 (NIH 3T3 cells stably expressing mutated Src where the tyrosine 527 is replaced by phenylalanine), and Src*3T3/CMS (Src*3T3 fibroblasts stably expressing Myc-tagged CMS) cells were cultured in Dulbecco's modified Eagle's medium (DMEM) supplemented with 5% calf serum. CMS expressing podocytes and Src*3T3/CMS fibroblasts were generated by retroviral infection as described (Kirsch et al., 2001). Conditionally immortalized mouse podocytes (gift from P. Mundel, Albert Einstein College of Medicine, New York, NY) were cultured at non-permissive temperature (33°C) in RPMI-1640 medium supplemented with 10% fetal bovine serum (FBS) and 10 ng/ml interferon γ (Life Technologies Inc.), or under permissive temperature (37°C) in medium lacking interferon γ.

Plasmid construction

The FLAG-tagged constructs CMS, CMS/TH and CMS/3SH3 have been described elsewhere (Kirsch et al., 1999). CMS/ΔPR was generated as described previously (Kirsch et al., 2001) and cloned in frame with the FLAG-tag into the pFLAG-CMV2 vector. CMS ΔCC, CMS 605 and CMS 628 were generated by site-directed mutagenesis using the QuickChange Kit (Stratagene Inc). Stop codons were introduced at positions Y548, E605, and R628, respectively. GST fusion constructs for mapping the actin-binding site on CMS were generated as follows: deletion constructs of CMS (CMS-CT, CT ΔPR, CT ΔΔ, CT 525-639, and CT 582-639) were amplified by PCR with customized primers, and cloned in frame with GST into pGEX6-P1 vector (Amersham Biosciences Corp.) using the *Bam*HI and *Eco*RI sites for cloning. The CT ΔCC was amplified by PCR using the FLAG-taged CMS ΔCC construct described above as template. The CT 524 construct was generated by site directed mutagenesis using the pGEX6-P1 CMS-CT construct described above as template. We introduced stop codons at Y548 and E525, respectively. The CT PR/CC construct was generated by linking the proline-rich region (PR, K346-P422) to the coiled-coil domain (CC, S582-S639). The GST-talin plasmid was generated by PCR amplification of the actin-binding domain of murine talin (I2,347-H2,541) and insertion into the pGEX6P-1 vector using GFP-talin as template (gift from Benedikt Kost, The Rockefeller University, New York, NY). CIN85-CT, (P357-K665) and CIN85 ΔPR (T432-K665), were amplified by PCR from a BT20 cell cDNA library, and inserted into the *Bam*HI and *Xho*I sites of pGEX6P-1. Amino acid numbers for CIN85 are based on the full-length protein (accession number AF230904). The CMS-CIN85 hybrid was generated by sequential cloning of the DNA sequences encoding the PR region of CMS, the linker region of CIN85 (T432-P601), and the CC domain of CMS into the pGEX6P-1 vector. To facilitate the cloning, an *Xho*I restriction site was introduced for linking the cDNA of the PR region with cDNA of the linker region. Similarly, a *Not*I site was introduced for linking the CIN85 linker region with the CC domain. All PCR products and junctions were verified by DNA sequencing.

Transfection of siRNA

For the CMS repression studies, the *CD2AP* siRNA pool of three target specific 20-25 nucleotides was used (sc-29985; Santa Cruz Biotechnology, Santa Cruz, CA). Transfections (*CD2AP* siRNA: 80 nM and 160 nM final concentration; control siRNA 80 nM) were carried out using Oligofectamine (Invitrogen, Carlsbad, CA), in OPTI-MEM serum-free medium, 24 hours after plating.

Migration assays

Suspensions of 1×10^5 podocytes with reduced CMS and, podocytes and Src*3T3 cells carrying CMS or mutant constructs were layered in the upper compartment of a Transwell (Costar, Cambridge, MA) on an 8-mm diameter polycarbonate filter (8 μm pore size), and incubated at 37°C for the indicated times as descibed (Belguise et al., 2005). Migration of the cells to the lower side of the filter was evaluated by crystal violet staining (0.2% crystal violet, 10% ethanol) for 10 minutes. The dye was removed, and the wells were washed three times with ddH_2O. Finally 200 μl of solubilization buffer (2% SDS in PBS) per well was added and incubated at RT for 10 minutes and the OD_{550} determined.

RT-PCR analysis

Total RNA of mouse podocytes was extracted using Trizol according to the protocol (Invitrogen). Subsequently, 2 μg RNA was transcribed into cDNA in a final volume of 25 μl using random primers and the Superscript II kit (Invitrogen). The N-terminus and C-terminus of full-length CIN85 were amplified by standard PCR (30 cycles) using 2 μl cDNA as template. The mouse CIN85 primers: m1 (5′-TTCCGCCAACTTTCACTCTG-3′), mmn (5′-GGCAGGAAGTCATTTTCCAC-3′), mc (5′-TTCACTTCCATCTGCAACCG-3′), were described (Buchman et al., 2002). The m6 primer: (5′-GGCATCCTGGATAAGGACCTC-3′). PCR products were purified and subjected to sequence analysis.

Immunofluorescence

Immunofluorescence on NIH 3T3, Src*3T3, Src*3T3/CMS and COS-7 cells was performed as described previously (Kirsch et al., 1999). Podocytes, stably expressing CMS were grown on collagen-coated coverslips. Cells were fixed with 3% formaldehyde-PBS for 30 minutes at RT, and permeabilized with 0.2% Triton X-100/PBS for 5 minutes. Nonspecific binding sites were blocked with 50 mM glycine/PBS for 10 minutes. Cells were stained with monoclonal anti-Myc antibody (Santa Cruz Inc; sc-40, 1:250) diluted in PBS-gelatin. After four washes, cells were incubated with FITC-donkey anti-mouse IgG and Rhodamine-phalloidin (Jackson Immunoresearch Laboratories and Molecular Probes, respectively; 1:300). COS-7 and Src*3T3 cells were inspected by confocal laser scanning microscopy (Carl Zeiss, LSM10). Podocytes and fibroblasts were inspected by fluorescence microscopy (Carl Zeiss, Axiovert 200M, Hamamatsu ORCA-ER camera).

Actin polymerization

Non-muscle G-actin (Cytoskeleton; APHL99) diluted in buffer A (5 mM Tris-HCl [pH 8.0], 0.2 mM $CaCl_2$, 0.2 mM ATP) to a final concentration of 1 mg/ml, and pre-cleared by centrifuging at 100,000 ***g***, at 4°C for 40 minutes. The pre-cleared G-actin was polymerized at a working concentration of 0.5 mg/ml, and used subsequently. The polymerization reaction was performed at RT for 30 minutes, in 1× polymerization buffer (50 mM KCl, 1 mM $MgCl_2$, 1 mM EGTA, 1 mM ATP, 0.025 mg/ml phalloidin, 1 mM DTT, 10 mM imidazole, pH 7.3) and used immediately.

Expression of GST fusion peptides, in vitro G-actin and F-actin binding assays

Expression and affinity purification of GST fusion proteins was carried out as described (Kirsch et al., 1998). Purified recombinant proteins were dialyzed against 1× F-actin binding buffer (FABB) (75 mM KCl, 5 mM $MgCl_2$, 10 mM imidazole, 1 mM EDTA, 0.2 mM DTT, 0.5 mM ATP, pH 7.2) supplemented with 0.1 mg/ml bovine serum albumin (BSA) [modified from Fanning et al. (Fanning et al., 1998)]. Protein quality was inspected by Coomassie stained gels. The images were captured with a Minolta DiMage5 camera, and for assay loading normalization, the bands corresponding to the full-length protein constructs were quantified with the ImageJ (NIH Image) program. For in vitro binding assays, G-actin or freshly polymerized F-actin at a final concentration of 3 μM was incubated with 0.3-0.5 μM (10 μg) GST-tagged purified recombinant protein, and 25 μl glutathione beads in a total volume of 600 μl 1 × FABB. The samples were incubated on a Nutator at 22°C for 2 hours. Subsequently, the beads were washed four times with 1 ml 1 × FABB-BSA by centrifuging at 400 ***g*** for 5 minutes. Pellets were resuspended in 100 μL SDS-PAGE sample buffer; 50 μl reactions were subjected to SDS-PAGE. Western blotting was performed as described (Kirsch et al., 1998) with anti-actin antibody (C-2, Santa Cruz Inc.). Bands were analyzed by densitometry using an Identity Multiscan instrument (Molecular Dynamics Inc.).

In vivo F-actin co-sedimentation assay

The assay was performed as described (Fanning et al., 1998). Briefly, 293T cells plated into 100-mm dishes were transfected with FLAG-tagged CMS constructs (CMS, CMS/3SH3, CMS/TH, CMS/ΔCC, and CMS/ΔPR) and with GFP-tagged talin as described (Kirsch et al., 1998). After 48 hours, the cells were washed twice with PBS and scraped on ice into 1.0 ml of a hypotonic lysis buffer [10 mM sodium carbonate (pH 11.0), 1.0 mM K-EGTA, 5.0 mM $MgCl_2$, 0.2 mM DTT], and protease inhibitors. Cells were homogenized using a Dounce homogenizer. The resulting lysate was clarified at 100,000 ***g*** for 1 hour at 4°C, and the pH of the supernatant was adjusted to 7.0 by the addition of 9.0 μl of 1.0 M HCl and 20 μl of 1.0 M Tris-HCl (pH 7.0). Before being used in the co-sedimentation assay, the neutralized lysate was clarified again at 100,000 ***g*** for 1 hour at 4°C. A 55 μM stock of 10× F-actin was generated as follows, non-muscle G-actin stocks (10 mg/ml) (Cytoskeleton Inc.) were diluted in binding buffer resulting in a final concentration of 55 μM actin, 20 μM imidazole, (pH 7.2), 5 mM $MgCl_2$, 0.5 mM DTT, 75 mm KCl, 32 μM phalloidin (Molecular Probes), incubated for 30 minutes at RT. F-actin at a final concentration of 5.5 μM, was mixed with 60 μl of the cell lysates in binding buffer in a final volume of 200 μl and incubated at RT for 20 minutes. Samples were subsequently spun at 100,000 ***g*** at 22°C for 20 minutes. Western blotting with the anti-FLAG antibody and anti GFP antibody as described (Kirsch et al., 1998). The blots were stripped and reprobed with an anti-actin antibody.

F-actin bundling assay

Pre-cleared GST or GST-tagged fusion proteins were incubated in 1× FABB containing 25 μl protein-A sepharose beads at RT for 30 minutes. Subsequently, the mixtures were cleared by centrifugation at 16,000 ***g*** at 4°C for 30 minutes using a tabletop centrifuge, and the proteins were immediately used. The bundling reaction was performed as follows: 5 μg of pre-cleared GST or GST-tagged proteins (0.5-1.5 μM) and 50 μg of F-actin (7 μM) were mixed with 1× FABB supplemented with 0.1 mg/ml BSA, in a total volume of 160 μl, and incubated at RT for 30 minutes. Subsequently, F-actin bundles were pelleted at 16,000 ***g*** at 4°C for 30 minutes using a tabletop centrifuge. The supernatant was carefully removed, and the pellet was resuspended in 1 ml 1× FABB, and respun for 15 minutes. The wash step was repeated once. To visualize the pellet and to avoid it being suctioned away, 25 μl G150 sephadex beads slurry was added to the mix. Finally, the pellet was resuspended in 50 μl SDS-PAGE sample buffer, subjected to SDS-PAGE, and western blot analysis (described above).

Transmission electron microscopy

Pre-cleared purified recombinant GST proteins, and polymerized F-actin were prepared as described for the F-actin bundling assay. Protein samples, 0.7-2 μM (0.05 mg/ml) GST proteins, and 6 μM (0.25 mg/ml) for F-actin, were mixed in 1× FABB and incubated at RT for 30 minutes. Subsequently, 10 μl aliquots were applied to Formvar/carbon-coated grids (Ted Pella Inc.), and negatively stained with 2% phosphotungstic acid (pH 7.3). The grids were viewed using a Philips 300 electron microscope.

We are grateful to Vickery Trinkaus-Randall for help with the confocal microscopy, and Thomas Christensen for access to the electron microscope. This work was supported in part by grants from the American Cancer Society, the Basil O'Connor Starter Scholar Research Award Grant no. 5-FY01-452 from the March of Dimes Foundation, the NIH NCI CA106468 to K.H.K., and by NIH NIA AG00115.

References

Belguise, K., Kersual, N., Galtier, F. and Chalbos, D. (2005). FRA-1 expression level regulates proliferation and invasiveness of breast cancer cells. *Oncogene* **24**, 1434-1444.

Berger, B., Wilson, D. B., Wolf, E., Tonchev, T., Milla, M. and Kim, P. S. (1995). Predicting coiled coils by use of pairwise residue correlations. *Proc. Natl. Acad. Sci. USA* **92**, 8259-8263.

Bogler, O., Furnari, F. B., Kindler-Roehrborn, A., Sykes, V. W., Yung, R., Huang, H. J. and Cavenee, W. K. (2000). SETA: a novel SH3 domain-containing adapter molecule associated with malignancy in astrocytes. *Neuro-oncology* **2**, 6-15.

Borinstein, S. C., Hyatt, M. A., Sykes, V. W., Straub, R. E., Lipkowitz, S., Boulter, J. and Bogler, O. (2000). SETA is a multifunctional adapter protein with three SH3 domains that binds Grb2, Cbl, and the novel SB1 proteins. *Cell. Signal.* **12**, 769-779.

Brett, T. J., Traub, L. M. and Fremont, D. H. (2002). Accessory protein recruitment motifs in clathrin- mediated endocytosis. *Structure* **10**, 797-809.

Bruck, S., Huber, T. B., Ingham, R. J., Kim, K., Niederstrasser, H., Allen, P. M., Pawson, T., Cooper, J. A. and Shaw, A. S. (2006). Identification of a novel inhibitory actin capping protein binding motif in CD2 associated protein. *J. Biol. Chem.* **281**, 19196-19203.

Bruzzantini, A., Neff, L., Sanjay, A., Horne, W. C., DeCamilli, P. and Baron, R. (2005). Dynamin forms a Src kinase-sensitive complex with Cbl and regulates podosomes and osteoclast activity. *Mol. Biol. Cell* **16**, 3301-3313.

Buccione, R., Orth, J. D. and McNiven, M. A. (2004). Foot and mouth: podosomes, invadopodia and circular dorsal ruffles. *Nat. Rev. Mol. Cell Biol.* **5**, 647-657.

Buchman, V. L., Luke, C., Borthwick, E. B., Gout, I. and Ninkina, N. (2002). Organization of the mouse Ruk locus and expression of isoforms in mouse tissues. *Gene* **295**, 13-17.

Chen, B., Borinstein, S. C., Gillis, J., Sykes, V. W. and Bogler, O. (2000). The glioma-associated protein SETA interacts with AIP1/Alix and ALG-2 and modulates apoptosis in astrocytes. *J. Biol. Chem.* **275**, 19275-19281.

Cormont, M., Metón, I., Mari, M., Monzo, P., Keslair, F., Gaskin, C., McGraw, T. E. and Le Marchand-Brustel, Y. (2003). CD2AP/CMS regulates endosome morphology and traffic to the degradative pathway through its interaction with Rab4 and c-Cbl. *Traffic* **4**, 97-112.

Destaing, O., Saltel, F., Geminard, J. C., Jurdic, P. and Bard, F. (2003). Podosomes display actin turnover and dynamic self-organization in osteoclasts expressing actin-green fluorescent protein. *Mol. Biol. Cell* **14**, 407-416.

Dikic, I. (2002). CMS/CIN85 family of adaptor molecules. *FEBS Lett.* **529**, 110-115.

Dustin, M. L., Olszowy, M. W., Holdorf, A. D., Li, J., Bromley, S., Desai, N., Widder, P., Rosenberger, F., van der Merwe, P. A., Allen, P. M. et al. (1998). A novel adaptor protein orchestrates receptor patterning and cytoskeletal polarity in T-cell contacts. *Cell* **94**, 667-677.

Fanning, A. S., Jameson, B. J., Jesaitis, L. A. and Anderson, M. J. (1998). The tight junction protein ZO-1 establishes a link between the transmembrane protein occludin and the actin cytoskeleton. *J. Biol. Chem.* **273**, 29745-29753.

Ferrary, E., Cohen-Tannoudji, M., Pehau-Arnaudet, G., Lapillonne, A., Athman, R., Ruiz, T., Boulouha, L., El Marjou, F., Doye, A., Fontaine, J. J. et al. (1999). In vivo, villin is required for Ca(2+)-dependent F-actin disruption in intestinal brush borders. *J. Cell Biol.* **146**, 819-830.

Gout, I., Middleton, G., Adu, J., Ninkina, N. N., Drobot, L. B., Filonenko, V., Matsuka, G., Davies, A. M., Waterfield, M. and Buchman, V. L. (2000). Negative regulation of PI 3-kinase by Ruk, a novel adaptor protein. *EMBO J.* **19**, 4015-4025.

Hutchings, N. J., Clarkson, N., Chalkley, R., Barclay, A. N. and Brown, M. H. (2003). Linking the T cell surface protein CD2 to the actin-capping protein CAPZ via CMS and CIN85. *J. Biol. Chem.* **278**, 22396-22403.

Kaksonen, M., Toret, C. P. and Drubin, D. G. (2006). Harnessing actin dynamics for clathrin-mediated endocytosis. *Nat. Rev. Mol. Cell Biol.* **7**, 404-414.

Kirsch, K. H., Georgescu, M. M. and Hanafusa, H. (1998). Direct binding of p130(Cas) to the guanine nucleotide exchange factor C3G. *J. Biol. Chem.* **273**, 25673-25679.

Kirsch, K. H., Georgescu, M. M., Ishimaru, S. and Hanafusa, H. (1999). CMS: an adapter molecule involved in cytoskeletal rearrangements. *Proc. Natl. Acad. Sci. USA* **96**, 6211-6216.

Kirsch, K. H., Georgescu, M. M., Shishido, T., Langdon, W. Y., Birge, R. B. and Hanafusa, H. (2001). The adapter type protein CMS/CD2AP binds to the proto-oncogenic protein c-Cbl through a tyrosine phosphorylation-regulated Src homology 3 domain interaction. *J. Biol. Chem.* **276**, 4957-4963.

Kobayashi, S., Sawano, A., Nojima, Y., Shibuya, M. and Maru, Y. (2004). The c-Cbl/CD2AP complex regulates VEGF-induced endocytosis and degradation of Flt-1 (VEGFR-1). *FASEB J.* **18**, 929-931.

Kowanetz, K., Husnjak, K., Höller, D., Kowanetz, M., Soubeyran, P., Hirsch, D.,

Schmidt, M., Pavelic, K., De Camilli, P., Randazzo, P. et al. (2004). CIN85 associates with multiple effectors controlling intracellular trafficking of epidermal growth factor receptors. *Mol. Biol. Cell* **15**, 3155-3166.

Lehtonen, S., Ora, A., Olkkonen, V. M., Geng, L., Zerial, M., Somlo, S. and Lehtonen, E. (2000). In vivo interaction of the adapter protein CD2-associated protein with the type 2 polycystic kidney disease protein, polycystin-2. *J. Biol. Chem.* **275**, 32888-32893.

Lehtonen, S., Zhao, F. and Lehtonen, E. (2002). CD2-associated protein directly interacts with the actin cytoskeleton. *Am. J. Physiol. Renal Physiol*. **283**, F734-F743.

Linder, S. and Kopp, P. (2005). Podosomes at a glance. *J. Cell. Sci.* **118**, 2079-2082.

Liu, M., Chen, Y. and Sui, S. F. (2006). The identification of a new actin-binding region in p57. *Cell Res.* **16**, 106-112.

Lynch, D. K., Winata, S. C., Lyons, R. J., Hughes, W. E., Lehrbach, G. M., Wasinger, V., Corthals, G., Cordwell, S. and Daly, R. J. (2003). A Cortactin-CD2-associated protein (CD2AP) complex provides a novel link between epidermal growth factor receptor endocytosis and the actin cytoskeleton. *J. Biol. Chem*. **278**, 21805-21813.

Marchisio, P. C., Cirillo, D., Teti, A., Zambonin-Zallone, A. and Tarone, G. (1987). Rous sarcoma virus- transformed fibroblasts and cells of monocytic origin display a peculiar dot-like organization of cytoskeletal proteins involved in microfilament-membrane. *Exp. Cell Res.* **169**, 202-214.

Matsudaira, P. (1991). Modular organization of actin crosslinking proteins. *Trends Biochem. Sci.* **16**, 87-92.

Meyer, R. K. and Aebi, U. (1990). Bundling of actin filaments by alpha-actinin depends on it molecular length. *J. Cell Biol*. **110**, 2013-2024.

Monzo, P., Gauthier, N. C., Keslair, F., Loubat, A., Field, C. M., Le Marchand-Brustel, Y. and Cormont, M. (2005). Clues to CD2-asociated protein involvement in cytokinesis. *Mol. Biol. Cell* **16**, 2891-2902.

Nam, J. M., Onodera, Y., Mazaki, Y., Miyoshi, H., Hashimoto, S. and Sabe, H. (2007). CIN85, a Cbl-interacting protein, is a component of AMAP1-mediated breast cancer invasion machinery. *EMBO J*. **26**, 647-656.

Ochoa, G. C., Slepnev, V. I., Neff, L., Ringstad, N., Takei, K., Daniell, L., Kim, W., Cao, H., McNiven, M., Baron, R. et al. (2000). A functional link between dynamin and the actin cytoskeleton at podosomes. *J. Cell Biol.* **150**, 377-389.

Petrelli, A., Gilestro, G. F., Lanzardo, S., Comoglio, P. M., Migone, N. and Giordano, S. (2002). The endophilin-CIN85-Cbl complex mediates ligand-dependent downregulation of c-Met. *Nature* **416**, 187-190.

Schmidt, M. H., Chen, B., Randazzo, L. M. and Bogler, O. (2003). SETA/CIN85/Ruk and its binding partner AIP1 associate with diverse cytoskeletal elements, including FAKs, and modulate cell adhesion. *J. Cell Sci.* **116**, 2845-2855.

Schmidt, M. H., Dikic, I. and Bogler, O. (2005). Src phosphorylation of Alix/AIP1 modulates its interaction with binding partners and antagonizes its activities. *J. Biol. Chem.* **280**, 3414-3425.

Shih, N., Li, J., Karpitskii, V., Nguyen, A., Dustin, M., Kanagawa, O., Miner, J. and Shaw, A. (1999). Congenital nephrotic syndrome in mice lacking CD2-associated protein. *Science* **286**, 312-315.

Soubeyran, P., Kowanetz, K., Szymkiewicz, I., Langdon, W. Y. and Dikic, I. (2002). Cbl-CIN85-endophilin complex mediates ligand-induced downregulation of EGF receptors. *Nature* **416**, 183-187.

Take, H., Watanabe, S., Takeda, K., Yu, Z. X., Iwata, N. and Kajigaya, S. (2000). Cloning and characterization of a novel adaptor protein, CIN85, that interacts with c-Cbl. *Biochem. Biophys. Res. Commun.* **268**, 321-328.

Tibaldi, E. V. and Reinherz, E. L. (2003). CD2BP3, CIN85 and the structurally related adaptor protein CMS bind to the same CD2 cytoplasmic segment, but elicit divergent functional activities. *Int. Immunol.* **15**, 313-329.

Welsch, T., Endlich, N., Kriz, W. and Endlich, K. (2001). CD2AP and p130Cas localize to different F-actin structures in podocytes. *Am. J. Physiol. Renal Physiol*. **281**, F769-F777.

Welsch, T., Endlich, N., Gokce, G., Doroshenko, E., Simpson, J. C., Kriz, W., Shaw, A. S. and Endlich, K. (2005). Association of CD2AP with dynamic actin on vesicles in podocytes. *Am. J. Physiol. Renal Physiol.* **289**, F1134-F1143.

Yuan, H., Takeuchi, E., Taylor, G. A., McLaughlin, M., Brown, D. and Salant, D. J. (2002). Nephrin dissociates from actin, and its expression is reduced in early experimental membranous nephropathy. *J. Am. Soc. Nephrol.* **13**, 946-956.

Journal of Cell Science